APRIL 1983 LIDS-P-1302

ROBUSTNESS OF CONTINUOUS-TIME ADAPTIVE CONTROL ALGORITHMS IN THE PRESENCE OF UNMODELED DYNAMICS*

by

Charles E. Rohrs, Lena Valavani, Michael Athans, and Gunter Stein
Laboratory for Information and Decision Systems
Massachusetts Institute of Technology
Cambridge, Massachusetts 02139

ABSTRACT

This paper examines the robustness properties of existing adaptive control algorithms to unmodeled plant high-frequency dynamics and unmeasurable output disturbances. It is demonstrated that there exist two infinite-gain operators in the nonlinear dynamic system which determines the time-evolution of output and parameter errors. The pragmatic implication of the existence of such infinite-gain operators is that (a) sinusoidal reference inputs at specific frequencies and/or (b) sinusoidal output disturbances at any frequency (including d.c.), can cause the loop gain to increase without bound, thereby exciting the unmodeled high-frequency dynamics, and yielding an unstable control system. Hence, it is concluded that existing adaptive control algorithms cannot be used with confidence in practical designs, because instability can result with high probability.

*Research supported by NASA Ames and Langley Research Centers under grant NASA/NGL-22-009-124, by the Office of Naval Research under grant ONR/N00014-82-K-0582(NR 606-003), and by the National Science Foundation under grant NSF/ECS-8210960.

1. INTRODUCTION

This paper reports the outcome of an exhaustive analytical and numerical investigation of the stability and robustness properties of a wide class of adaptive control algorithms in the presence of unmodeled high-frequency dynamics and persistent unmeasurable output disturbances. Every physical system has such (parasitic) high-frequency dynamics; in non-adaptive designs these limit the cross-over frequency and require good gain and phase margins. Also, every control system must be able to operate in the presence of unmeasured and possibly persistent disturbances without going unstable. In non-adaptive linear control designs the presence of disturbances does not impact upon the closed-loop stability issue.

It should be stressed that the existing adaptive control algorithms, when used to control an unknown linear time-invariant plant, result in a highly nonlinear and time-varying closed-loop system whose stability does depend upon the external inputs (reference inputs and disturbance inputs). Hence, it is important to analyze the stability of the adaptive closed-loop design and to inquire about its global stability properties. This has provided the motivation for the research reported in this paper.

Due to space limitations we cannot possibly provide in this paper analytical and simulation evidence of all conclusions outlined in the abstract. Rather, we summarize the basic approach only for a single class of continuous-time algorithms that includes those of Monopoli [14], Narendra and Valavani [1], and Feuer and Morse [2]. However, the same analysis techniques have been used to analyze more complex classes of (1) continuous-time adaptive control algorithms due to Narendra, Lin, and Valavani [3], both algorithms suggested by Morse [4], and the algorithms suggested by Egardt [7] which include those of Landau and Silveira [6], and Kreisselmeier [19]; and (2) discrete-time adaptive control algorithms due to Narendra and Lin [22] Goodwin, Ramadge, and

Caines [23] (the so-called dead-beat controllers), and those developed in Egardt [17], which include the self-tuning regulator of Åström and Wittenmark [18] and that due to Landau [20]. The thesis by Rohrs [15] contains the full analysis and simulation results for the above classes of existing adaptive algorithms.

The end of the 1970's marked significant progress in the theory of adaptive control, both in terms of obtaining global asymptotic stability proofs [1-7] as well as in unifying diverse adaptive algorithms, the derivation of which was based on different philosophical viewpoints [8,9].

Unfortunately, the stability proofs of all these algorithms have in common a very restrictive assumption. For continuous-time implementation this assumption is that the number of poles minus the number of zeroes of the plant, i.e. its relative degree, is known. The counterpart of this assumption for discrete-time systems is that the pure delay in the plant is exactly an integer number of sampling periods and that this integer is known. It is also assumed that an upper bound for the number of poles in the plant is known in both the continuous-time and discrete-time formulations. Finally, global parameter convergence requires that the inputs satisfy a "sufficiently rich" condition.

The restrictive relative degree assumption, in turn, is equivalent to enabling the designer to realize for an adaptive algorithm, a positive real error transfer function, on which all stability proofs have heavily hinged to-date [8]. Positive realness implies that the phase of the system cannot exceed $\pm 90°$ for all frequencies, while it is a well known fact that models of physical systems become very inaccurate in describing actual plant high-frequency phase characteristics. Moreover, for practical reasons, most controller designs need to be based on models which do not contain all of the plant dynamics, in order to keep the complexity of the required adaptive compensator within bounds.

Motivated from such considerations, researchers in the field recently started investigating the robustness of adaptive algorithms to violation of the restrictive (and unrealistic) assumption of knowledge of the plant order and its relative degree. Ioannou and Kokotovic [10] obtained error bounds for adaptive observers and identifiers in the presence of unmodeled dynamics, while such analytical results were harder to obtain for reduced order adaptive controllers. The first such result, obtained by Rohrs et.al. [11], consists of "linearization" of the error equations, under the assumption that the overall system is in its final approach to convergence. Ioannou and Kokotovic [12] later obtained local stability results in the presence of unmodeled dynamics, and showed that the speed ratio of slow versus fast (unmodeled) dynamics directly affected the stability region. Even the local stability results of [12] can only be attained when the speed ratio is small, i.e. when the unmodeled dynamics are much faster than the modeled part of the process. Earlier simulation studies by Rohrs et.al [13] had already shown increased sensitivity of adaptive algorithms to disturbances and unmodeled dynamics, generation of high frequency control inputs and ultimately instability. Simple root-locus type plots for the linearized system in [11] showed how the presence of unmodeled dynamics could bring about instability of the overall system. It was also shown there that the generated frequencies in the adaptive loop depend nonlinearly on the magnitudes of the reference input and output. Kosut and Friedlander [23] have also tried to define the class of plant perturbations under which adaptive controllers will retain stability; unfortunately, their characterization includes unmodeled dynamics by definition. They have also found similar limitations as in [11], on the reference input and output characteristics for which the linearized error equations are stable.

The main contribution of this paper is in showing that two operators inherently present in all algorithms considered -- as part of the adaptation mechanism -- have

infinite gain. As a result, two possible mechanisms of instability are isolated and discussed. It is argued that the destabilizing effects in the presence of unmodeled dynamics can be attributed to either phase -- in the case of high frequency inputs -- or, primarily, gain considerations -- in the case of unmeasurable output disturbances of any frequency, including d.c., which result in nonzero steady-state errors. The latter fact is most disconcerting for the performance of adaptive algorithms since it cannot be dealt with, given that a persistent disturbance of any frequency can have a destabilizing effect.

Our conclusions that the adaptive algorithms considered cannot be used for practical adaptive control, because the physical system will eventually become unstable, are based upon two facts of life that cannot be ignored in any physical control design: (1) there are always unmodeled dynamics at sufficiently high frequencies (and it is futile to try to model unmodeled dynamics) and (2) the plant cannot be isolated from unknown disturbances (e.g., 60 Hz hum) even though these may be small. Neither of these two practical issues have been included in the theoretical assumptions common to all adaptive algorithms considered, and this is why these algorithms cannot be used with confidence. Recent papers [12], [23] have addressed some of the relevant issues, but no complete answers are available. To avoid exciting unmodeled dynamics, stringent requirements must be placed upon the bandwidth and phase margin of the control loop; no such considerations have been discussed in the literature. It is not at all obvious, nor easy, how to modify or extend the available algorithms to control their bandwidth, much less their phase margin properties.

In Section 2 of this paper proofs for the infinite gain of the operators generic to the adaptation mechanism are given. Section 3 contains the development of two possible mechanisms for instability that arise as a result of the infinite gain operators. Simulation results that show the validity of the heuristic arguments in Section 3 are presented in Section 4. Section 5 contains the conclusions.

2. THE ERROR MODEL STRUCTURE FOR A REPRESENTATIVE ADAPTIVE ALGORITHM

The simplest prototype for a model reference adaptive control algorithm in continuous-time has its origins to at least as far back as 1974, in the paper by Monopoli [14]. This algorithm has been proven asymptotically stable only for the case when the relative degree of the plant is unity or at most two. The algorithms published by Narendra and Valavani [1] and Feuer and Morse [2] reduce to the same algorithm for the pertinent case. This algorithm will henceforth be referred to as CA1 (continuous-time algorithm No. 1).

The following equations summarize the dynamical equations that describe it; see also Figure 1. The equations presented here pertain to the case where a unity relative degree has been normally assumed. In the equations below, r(t) is the (command) reference input and the disturbance d(t) in Figure 1 is equal to zero.

Plant:
$$y(t) = \frac{g_p B(s)}{A(s)}\,[u(t)] \tag{1}$$

Auxiliary Variables:
$$w_{ui}(t) = \frac{s^{i-1}}{P(s)}\,[u(t)]; \quad i=1,2,\ldots,n-1 \tag{2}$$

$$w_{yi}(t) = \frac{s^{i-1}}{P(s)}\,[y(t)]; \quad i=1,2,\ldots,n \tag{3}$$

$$\underline{w}(t) \triangleq \begin{bmatrix} r(t) \\ \underline{w}_u(t) \\ \underline{w}_y(t) \end{bmatrix}; \quad \underline{k}(t) \triangleq \begin{bmatrix} k_r(t) \\ \underline{k}_u(t) \\ \underline{k}_y(t) \end{bmatrix} \tag{3a}$$

Model:
$$y_M(t) = \frac{g_M B_M(s)}{A_M(s)}\,[r(t)] \tag{4}$$

Control Input:
$$u(t) = \underline{k}^T(t)\underline{w}(t) = \underline{k}^{*T}(t)\underline{w}(t) + \tilde{\underline{k}}^T(t)\underline{w}(t) = \underline{k}^{*T}(t)\underline{w}(t) + \tilde{u}(t) \tag{5}$$

Output Error:
$$e(t) = y(t) - y_M(t) \tag{6}$$

Parameter Adjustment Law:
$$\dot{\underline{k}}(t) = \dot{\tilde{\underline{k}}}(t) = \underline{\Gamma}\,\underline{w}(t)e(t); \quad \underline{\Gamma} = \underline{\Gamma}' > \underline{0} \tag{7}$$

Nominal Controlled Plant:
$$\frac{g^*B^*}{A^*(s)} = \frac{k_r^* g_p B(s)P(s)}{A(s)P(s) - A(s)K_u^*(s) - g_p B(s)K_y^*(s)} \tag{8}$$

Error Equation:
$$e(t) = \left(\frac{g^*B^*(s)}{A^*(s)} - \frac{g_M B_M(s)}{A_M(s)}\right)[r(t)] + \frac{g^*B^*(s)}{A^*(s)}\left[\frac{\tilde{\underline{k}}^T(t)\underline{w}(t)}{k_r^*}\right] \tag{9}$$

In the above equations the following definitions apply:

$$\underline{k}(t) \triangleq \underline{k}^* + \tilde{\underline{k}}(t) \tag{10}$$

where $\underline{k}^*$ is a constant 2n vector.

$$K_u^*(s) \triangleq k_{u(n-1)}^* s^{n-2} + k_{u(n-2)}^* s^{n-3} + \ldots + k_{u1}^*$$

where k_{ui}^* is the i-th component of $\underline{k}_u^*$.

$$K_y^*(s) \triangleq k_{yn}^* s^{n-1} + k_{y(n-1)}^* s^{n-2} + \ldots + k_{y1}^* \ .$$

where k_{yi}^* is the i-th component of $\underline{k}_y^*$. In the preceding equations we have tried to preserve the conventional literature notation [3,4,5,9], with P(s) representing the characteristic polynomial for the state variable filters and $\tilde{\underline{k}}(t)$ the parameter misalignment vector. In Eqn. (8) $\frac{g^*B^*(s)}{A^*(s)}$ represents the closed-loop plant transfer function that would result if $\tilde{\underline{k}}$ were identically zero, i.e., if a constant control law $\underline{k}=\underline{k}^*$ were used. Under the conventional assumption that the plant relative degree is exactly known and, if $B_M(s)$ divides P(s), then $\underline{k}^*$ can be chosen [1], such that

$$\frac{g^*B^*(s)}{A^*(s)} = \frac{g_M B_M(s)}{A_M(s)} \tag{11}$$

If the relative degree assumption is violated, $\frac{g^*B^*(s)}{A^*(s)}$ can only get as close to $\frac{g_M B_M(s)}{A_M(s)}$ as the feedback structure of the controller allows. The first term on the right-hand side of eqn. (9) results from such a consideration. Note that if eqn.(11) were satisfied, eqn. (9) reduces to the familiar error equation form that has appeared in the literature [8] for exact modeling. For more details the reader is referred to the literature cited in this section as well as to [15].

Figure 2 represents in block diagram form the combination of parameter adjustment law and error equations described by eqns. (7) and (9).

In general, existing continuous-time algorithms [1] to [9] can be classified into four groups labeled here and in [15] as CA1, CA2, CA3, CA4 respectively for Continuous-Time Algorithms 1,2,3,4. Figure 3 represents a generalized error structure which can be particularized to describe the error loop of any one of the existing adaptive algorithms, both in continuous time and -by its discrete analog - in discrete time as well. In Figure 3, the forward loop consists of a positive real transfer function, while the feedback path comprises the adaptation mechanism (parameter adjustment), which contains the infinite gain operator(s). In the figure, the error system input $\tilde{u}(t)$ is synthesized according to

$$\tilde{u}(t) = \underline{\tilde{k}}^T(t)\underline{C}[y(t),u(t)]$$

where

$\underline{C}$: is a linear time-invariant system representing an observer or an auxiliary state generator.

$\underline{M}$: is usually a memoryless map, often the identify map.

$\underline{D}$: is a linear time-invariant system analogous to $\underline{C}$ and often identical to it.

$\underline{F}(s)$: a stable transfer function, often the identity.

$\underline{\tilde{k}}(t), \underline{\tilde{f}}(t)$: parameter error vectors related by $\underline{\tilde{k}}(t) = \underline{M}[\underline{\tilde{f}}(t)]$.

The above mentioned four classes of adaptive algorithms have in common the error feedback loop structure and the basic ingredients of the parameter update mechanism, i.e. multiplication-integration-multiplication, which forms the feedback part of the loop and is shown [15] to constitute the infinite gain operators present in all existing adaptive algorithms. These operators are shown in Fig. 5 as they apply specifically to CA2, CA3, CA4. Analogously, the discrete-time algorithms are classified into three distinct groups, DA1, DA2, DA3. The four classes mentioned in the preceding differ in the specific parameterization that realizes the positive real transfer function in the forward path and in the particular details of the parameter adjustment laws [choice of $\underline{C}$, $\underline{D}$, $\underline{M}$, $\underline{F}(s)$]. For example, in the simplest class of continuous-time adaptive algorithms (CA1), under perfect modeling, the forward transfer function represents the reference model transfer function, which the controlled plant is able to match exactly, by assumption [eqn. (11)]. Unfortunately, when unmodeled dynamics are present, the controlled plant can only match the reference model only up to a certain frequency range and thus, the forward loop transfer function, which represents the nominally controlled plant and determines the error dynamics, loses its positive realness property. This, in conjunction with the infinite gain operator(s) in the feedback loop can bring about instability.

3. THE INFINITE GAIN OPERATORS

3.1 Quantitative Proof of Infinite Gain for Operators of CAl

The error system in Fig. 2 consists of a forward linear time-invariant operator representing the nominal controlled plant complete with unmodeled dynamics, $\frac{g^*B^*}{k_r^*A^*}$, and a time-varying feedback operator. It is this feedback operator which is of immediate interest. The operator, reproduced in Fig. 4 for the case where $\underline{w}$ is a scalar and $\Gamma=1$, is parameterized by the function w(t) and can be represented mathematically as:

$$\tilde{u}(t) = G_{w(t)}[e(t)] = \tilde{u}_o + w(t)\int_0^t w(\tau)e(\tau)d\tau \tag{12}$$

In order to make the notion of the gain of the operator $G_w(t)\ [\cdot]$ precise, we introduce the following operator theoretic concepts.

Definition 1: A function f(t) from $[0,\infty)$ to R is said to be in L_{2e} if the truncated norm

$$||f(t)||_{L_2}^T \triangleq \left(\int_0^t f^2(\tau)d\tau\right)^{1/2} \tag{13}$$

is finite for all finite T.

Definition 2: The gain of an operator G[f(t)], which maps function in L_{2e} into functions in L_{2e} is defined as

$$||G|| = \sup_{\substack{f(t)\in L_{2e} \\ T\in[0,\infty)}} \frac{||G[f(t)]||_{L_2}^T}{||f(t)||_{L_2}^T} \tag{14}$$

If there is no finite number satisfying eqn. (14), then G is said to have infinite gain.

Theorem 1: If w(t) is given by

$$w(t) = b+c\ \sin\omega_o t \tag{15}$$

for any positive constants b,c,ω_o, the operator of eqn. (12) has infinite gain.

Proof: The proof consists of constructing a signal e(t), such that

$$\lim_{T\to\infty} \frac{||G_w[e(t)]||_{L_2}^T}{||e(t)||_{L_2}^T} \tag{16}$$

is unbounded.

Let $e(t) = a\ \sin(\omega_o t+\phi)$ with a an arbitrary positive constant, ϕ an arbitrary phase shift and ω_o the same constant as in eqn. (15). These signals produce:

$$w(t)e(t) = ab(\sin\omega_o t\ \cos\phi + \cos\omega_o t\ \sin\phi) + \tag{17}$$
$$+ ac\sin\omega_o t(\sin\omega_o t\ \cos\phi + \cos\omega_o t\ \sin\phi)$$

$$\tilde{k}(t) \triangleq \tilde{k}_o + \int_o^t w(t)e(\tau)d\tau =$$

$$= \tilde{k}_o + \frac{1}{2}\ ac\ \cos\phi\ \cdot t + \frac{1}{4}\ \frac{ac}{\omega_o}\ \sin\phi + \frac{abc\cos\phi}{\omega_o} +$$

$$+ \frac{ab}{\omega_o}\ \sin\phi\ \sin\omega_o t - \frac{ab}{\omega_o}\ \cos\phi\ \cos\omega_o t$$

$$- \frac{ac}{4\omega_o}\ \cos\phi\ \sin 2\omega_o t - \frac{ac}{4\omega_o}\ \sin\phi\ \cos 2\omega_o t \tag{18}$$

$$\tilde{u}(t) = G_w(t)[e(t)] = \tilde{u}_o + w(t) \int_o^t w(\tau)e(\tau)d\tau =$$

$$= \tilde{u}_o + \frac{3abc}{4\omega_o}\ \sin\phi + \frac{ab^2}{\omega_o}\ \cos\phi + \frac{\cos\phi}{2}\ (abc+ac^2\sin\omega_o t)t +$$

$$+ \left[\frac{ac^2}{4\omega_o} + \frac{ab^2}{\omega_o}\right]\ \sin\phi\ \sin\omega_o t - \frac{ab^2}{\omega_o}\ \cos\phi\ \cos\omega_o t + \frac{abc}{\omega_o}\ \cos\phi\ \sin\omega_o t$$

$$- \frac{3}{4}\ abc\ \cos\phi\ \sin 2\omega_o t - \frac{3}{4}\ abc\ \sin\phi\ \cos 2\omega_o t$$

$$- \frac{ac^2}{4\omega_o}\left[\cos\phi\ \sin\omega_o t\ \sin 2\omega_o t + \sin\phi\ \sin\omega_o t\ \cos 2\omega_o t\right] \tag{19}$$

Next, using standard norm inequalities, we obtain from eqn. (19)

$$||\tilde{u}(t)||_{L_2}^T \geq ||\frac{abc}{2} \cos\phi \cdot t + \frac{ac^2 t}{2} \cos\phi \sin\omega_o t||_{L_2}^T$$

$$- ||\tilde{u}_o||_{L_2}^T - ||\frac{ab}{\omega_o} (\frac{3c \sin\phi}{4} + a \cos\phi)||_{L_2}^T$$

$$- ||\frac{(ab^2}{\omega_o} + \frac{ac^2)}{4\omega_o} \sin\phi \sin\omega_o t||_{L_2}^T - ||\frac{ab^2}{\omega_o} \cos\phi \cos\omega_o t||_{L_2}^T$$

$$- ||\frac{abc}{\omega_o} \cos\phi \sin\omega_o t||_{L_2}^T - ||\frac{3}{4} \frac{abc}{\omega_o} \cos\phi \sin 2\omega_o t||_{L_2}^T$$

$$- ||\frac{3}{4} \frac{abc}{\omega_o} \sin\phi \cos 2\omega_o t||_{L_2}^T - ||\frac{ac^2}{2\omega_o} \cos\phi \cos\omega_o t||_{L_2}^T$$

$$- ||\frac{ac^2}{2\omega_o} \cos\phi \cos^3\omega_o t||_{L_2}^T - ||\frac{ac^2}{4\omega_o} \sin\phi \sin\omega_o t||_{L_2}^T$$

$$- ||\frac{ac^2}{2\omega_o} \sin\phi \sin^3\omega_o t||_{L_2}^T > \tag{20}$$

$$> ||\frac{1}{2} abc\, t \cos\phi + \frac{1}{2} ac^2 t \sin\omega_o t||_{L_2}^T - (K_1' T)^{1/2} \tag{21}$$

with

$$K_1' = \tilde{u}_o^2 + \left\{ \frac{ab}{\omega} \frac{(3c+a)}{4} \right\}^2 + \left(\frac{ab^2}{\omega_o} + \frac{ac^2}{4\omega_o} \right)^2 + \left(\frac{ab^2}{\omega_o} \right)^2 +$$

$$+ \left(\frac{abc}{\omega_o} \right)^2 + 2\left(\frac{3}{4} \frac{abc}{\omega_o} \right)^2 + 2\left(\frac{ac^2}{2\omega_o} \right)^2 + 2\left(\frac{ac^2}{4\omega_o} \right)^2 < \infty \tag{22}$$

Now

$$\left\{ ||\frac{1}{2} abc\, t \cos\phi + \frac{1}{2} ac^2 t \cos\phi \sin\omega_o t||_{L_2}^T \right\}^2 =$$

$$= \int_o^T \left(\frac{a^2 b^2 c^2 t^2 \cos^2\phi}{4} + \frac{a^2 c^4 t^2 \cos^2\phi \sin^2\omega_o t}{4} + \frac{a^2 bc^3 t^2 \cos^2\phi \sin\omega_o t}{2} \right) dt \tag{23}$$

$$= \left[\frac{a^2b^2c^2\cos^2\phi}{12}\, t^3\right]_0^T + \frac{a^2c^4\cos^2\phi}{4\omega_o^2}\left[\frac{(\omega_o t)^3}{6\omega_o} - \left\{\frac{(\omega_o t)^2}{\omega_o} + \frac{4}{\omega_o}\right\}\sin 2\omega_o t - 8\,\omega_o^2 t\,\cos\omega_o t\right]_0^T +$$

$$+ \frac{a^2bc^3\cos^2\phi}{2\omega_o^2}\left[(2-\omega_o t^2)\cos\omega_o t + 2t\,\sin\omega_o t\right]_0^T \tag{24}$$

$$\geq \left(\frac{a^2b^2c^2\cos^2\phi}{12} + \frac{a^2c^4\cos^2\phi}{24}\right)T^3 - K_2T^2 - K_1T - K_o \tag{25}$$

where

$$K_2 = \frac{a^2c^4\cos^2\phi}{4\omega_o} + \frac{a^2bc^3\cos^2\phi}{2\omega_o} < \infty \tag{26}$$

$$K_1 = 2a^2c^4\cos^2\phi + \frac{a^2bc^3}{\omega_o^2} < \infty \tag{27}$$

$$K_o = \frac{a^2c^4\cos^2\phi}{\omega_o^3} + \frac{a^2bc^3\cos^2\phi}{\omega_o^2} < \infty \tag{28}$$

Combining inequalities (21) and (25) we arrive at:

$$\left(||\tilde{u}(t)||_{L_2}^T\right)^2 \geq \left(\frac{a^2b^2c^2\cos^2\phi}{12} + \frac{a^2c^4\cos^2\phi}{24}\right)T^3 - K_2T^2 - K_1T - T_o \tag{29}$$

Also

$$\left\{||e(t)||_{L_2}^T\right\}^2 = a^2\int_0^T \sin 2\omega_o t\, dt \leq a^2T \tag{30}$$

Therefore,

$$\frac{||\tilde{u}(t)||_{L_2}^T}{||e(t)||_{L_2}^T} \geq \left[\frac{a^2b^2c^2\cos^2\phi}{12} + \frac{a^2c^4\cos^2\phi}{24}\left(T^3 - K_2T^2 - K_1T - K_o\right)\right]^{1/2} \xrightarrow{T\to\infty} \infty$$

and therefore, G_w for w as in eqn. (15) has infinite gain.

In addition to the fact that the operator $G_w(t)$ from e(t) to $\tilde{u}(t)$ has infinite gain, the operator H_w, from e(t) to $\tilde{k}(t)$ in Fig. 3 also has infinite gain. This operator is described by:

$$H_{w(t)}[e(t)] = \tilde{k}_o + \int_0^t w(\tau)e(\tau)d\tau \tag{31}$$

Theorem 2: The operator $H_{w(t)}$ with w(t) given in eqn. (15) has infinite gain.

Proof: Choose $e(t) = a \sin\omega_o t$ as before. Then $\tilde{k}(t) = H_{w(t)}[e(t)]$ is given by eqn. (18). Proof of infinite gain for this operator then follows in exactly analogous steps as in Theorem 1 and is, therefore, omitted.

Remark 1: Both operators G_w and H_w will also have infinite gain for vectors $\underline{w}(t)$, since the operators' infinite gains can arise from any component of the vector $\underline{w}(t)$.

3.2 Two Mechanisms of Instability

In this section, we use the algorithm CA1 to introduce and delineate two mechanisms which may cause unstable behavior in the adaptive system CA1, when it is implemented in the presence of unmodeled dynamics and excited by sinusoidal reference inputs or by disturbances. The arguments made for CA1 are also valid for other classes of algorithms mentioned in Section 2, mutatis mutandis. Since the arguments explaining instability are somewhat heuristic in nature, they are verified by simulation. Representative simulation results are given in Section 4.

3.2.1 The Cause of Possible Instability

In order to demonstrate the infinite gain nature of the feedback operator of the error system of CA1 in Section 2, it is assumed that a component of $\underline{w}(t)$ has the form

$$w_i(t) = b + c \sin\omega_o t \tag{32}$$

and that the error has the form

$$e(t) = a \sin(\omega_o t+\phi) \tag{33}$$

The arguments of Section 2 indicate that, if e(t) and a component of $\underline{w}(t)$ have distinct sinusoids at a common frequency, the operator $G_{\underline{w}(t)}$ of eqn. (12) and the operator $H_{\underline{w}(t)}$ of eqn. (31) will have infinite gains. Two possibilities for e(t) $\underline{w}(t)$ to have the forms of eqn. (32) and eqn. (33) are now considered.

Case 1: If the reference input consists of a sinusoid and a constant, e.g.

$$r(t) = r_1 + r_2 \sin\omega_o t \tag{34}$$

where r_1 and r_2 are constants, then the plant output y(t) will contain a constant term and a sinusoid at frequency ω_o with an arbitrary phase shift ϕ. Consequently, through eqns. (2), (3) and (3a), all components of the vector $\underline{w}(t)$ will contain a constant and a sinusoid of frequency ω_o, with a phase shift.

If the controlled plant matches the model at d.c. but not at the frequency ω_o, the output error

$$e(t) = y(t) - y_M(t) \tag{35}$$

will contain a sinusoid at frequency ω_o. Thus, the conditions for infinite gain in the feedback path of Figure 1 have been attained.

Case 2: If a sinusoidal disturbance, d(t), at frequency ω_o enters the plant output as shown in Fig. 1, the sinusoid will appear in $\underline{w}(t)$ through the following equation, which replaces eqn. (3) in the presence of an output disturbance:

$$w_{yi}(t) = \frac{s^{i-1}}{P(s)} [y(t)+d(t)]; \quad i=1,2,\ldots,n \tag{36}$$

The following equation replaces eqn. (6) when an output disturbance is present

$$e(t) = y(t) + d(t) - y_M(t) \tag{37}$$

Any sinusoid present in d(t) will also enter e(t) through eqn. (37). Thus the signals e(t) and $\underline{w}(t)$ will contain sinusoids of the same frequency and the operators $H_{\underline{w}(t)}$ and $G_{\underline{w}(t)}$ will display an infinite gain.

3.2.2 Instability Due to the Gain of the Operator $G_{\underline{w}}$ of Equation (12)

The operator $G_{\underline{w}}$ of eqn. (12) is not only an infinite gain operator but its gain influences the system in such a manner as to allow arguments using linear systems concepts, as outlined below.

Assume, initially, that the error signal is of the form of eqn. (33), i.e., a sinusoid at frequency ω_o. Assume also that a component of $\underline{w}(t)$ is of the form of eqn. (32), i.e., a constant plus a sinusoid at the same frequency ω_o as the input. The output of the infinite gain operator, $G_{\underline{w}(t)}$ of eqn. (12), as given by eqn. (19), consists of a sinusoid at frequency ω_o with a gain which increases linearly with time plus other terms at 0 radians/sec (i.e. d.c.) and other harmonics of ω_o; i.e. $\tilde{u}(t) = \frac{1}{2} ac^2 t \sin\omega_o t \cos\phi$ + other terms.

The infinite gain operator manifests its large gain by producing at the output a sinusoid at the same frequency, ω_o, as the input sinusoid but with an amplitude increasing with time. By concentrating on the signal at frequency ω_o, and viewing the operator $G_{\underline{w}(t)}$ as a simple time-increasing gain with no phase shift at the frequency ω_o, and very small gain at other frequencies, we will be able to come up with a mechanism for instability of the error system of Figure 2, where $G_{w(t)}$ consists of the feedback part of the loop. If the foward path, $\frac{g^*B^*(s)}{k_r^*A^*(s)}$, of the error loop of

Figure 2, has less than $\pm 180°$ phase shift at the frequency ω_o, and if the gain of $G_{\underline{w}(t)}$ were indeed small at all other frequencies, then the high gain of $G_{\underline{w}(t)}$ at ω_o would not affect the stability of the error loop. If, however, the forward loop, $\frac{g^*B^*(s)}{k_r^*A^*(s)}$ does have 180° phase shift at ω_o, the combination of this phase shift with the sign reversal will produce a positive feedback loop around the operator $G_{\underline{w}(t)}$, thereby reinforcing the sinusoid at the input of $G_{\underline{w}(t)}$. The sinusoid will then increase in amplitude linearly with time, as the gain of $G_{\underline{w}(t)}$ grows, until the combined gain of $G_{\underline{w}(t)}$ and $\frac{g^*B^*(s)}{k_r^*A^*(s)}$ exceeds unity at the frequency ω_o. At his point, the loop itself will become unstable and all signals will grow without bound very quickly (as the effects of the unstable loop and continually growing gain of $G_{\underline{w}(t)}$ compound).

Since the infinite gain of $G_{\underline{w}(t)}$ can be achieved at any frequency ω_o, if $\frac{g^*B^*(s)}{k_r^*A^*(s)}$ has $\pm 180°$ phase shift at any frequency, the adaptive system is susceptible to instability from either a reference input or a disturbance.

Thus the importance of the Relative Degree Assumption, which essentially allows one to assume that $\frac{g^*B^*(s)}{k_r^*A^*(s)}$ is strictly positive real is seen. The stability proof CA1 hinges on the assumption that $\frac{g^*B^*(s)}{k_r^*A^*(s)}$ is strictly positive real and that $G_{\underline{w}(t)}$ is passive, i.e.

$$\int_0^\infty G_{w(t)}[e(t)]e(t)dt \geq 0 \ . \tag{38}$$

Both properties of positive realness and passivity are properties which are independent of the gain of the operator involved. However, it is always the case that, due to the inevitable unmodeled dynamics, only a bound is known on the gain of the plant at high frequencies. Therefore, for a large class of unmodeled dynamics with relative

degree two or greater, the operator, $\frac{g^*B^*}{k^*A^*_r}$, will have $\pm 180°$ phase shift at some frequency and be susceptible to unstable behavior if subjected to sinusoidal reference inputs and/or disturbances in that frequency range.

3.2.3 Instability Due to the Gain of the Operator H_w of Equation (31)

In the previous subsection, the situation was examined where the amplitude of the sinusoidal error e(t) grew with time due to a positive feedback mechanism in the error loop. In this subsection, we explore the situation where the sinusoidal error, e(t), is not at a frequency where it will grow due to the error system but, rather, when there exist persistent steady-state errors. Such a persistent error could arise from either or both of the two mechanisms discussed in Section 3.1.

1) A reference input with a number of frequencies is applied and the controlled plant with unmodeled dynamics cannot match the model in amplitude and phase for all reference input frequencies involved. This will cause a persistent sinusoid in both the error e(t), through eqn. (6), and the signals $\underline{w}(t)$, through eqns. (2) and (3), and/or,

2) An output sinusoidal disturbance, d(t), enters as shown in Figure 1, causing the persistent sinusoid directly on e(t), through eqn. (37), and w(t) through eqn. (36).

Assume that, through one of the above or any other mechanism, a component of $\underline{w}(t)$ contains a sinusoid at frequency ω_o as in eqn. (32) and that e(t) contains a sinusoid of the same frequency. Then the operator $H_{\underline{w}(t)}$ has infinite gain and the norm of the output signal of this operator, $\tilde{k}(t)$, increase without bound. The signal $\tilde{k}(t)$, will take the form of eqn. (18), repeated here:

$$\tilde{k}(t) = \tilde{k}_o + \frac{1}{2} act \cos\phi + \frac{1}{4} \frac{ac}{\omega_o} \sin\phi + \frac{ab\cos\phi}{\omega_o} +$$
$$+ \frac{ab}{\omega_o} \sin\phi \sin\omega_o t - \frac{ab}{\omega_o} \cos\phi \cos\omega_o t - \frac{ac}{4\omega_o} \cos\phi \sin 2\omega_o t$$
$$- \frac{ac}{4\omega_o} \sin\phi \cos 2\omega_o t$$

From the second term one can see that the parameters of the controller, defined in eqn. (10), i.e., $\underline{k}(t) = \underline{k}^* + \tilde{\underline{k}}(t)$, will increase without bound.

If there are any unmodeled dynamics at all, increasing the size of the nominal feedback controller parameters without bound will cause the adaptive system to become unstable. Indeed, since it is the gains of the nominal feedback loop that are unbounded, the system will become unstable for a large class of plants including all those whose relative degree is three or more, even if no unmodeled dynamics are present.

4. SIMULATION RESULTS

In this section the arguments for instability presented in the previous sections are shown to be valid via simulation.

The simulations were generated using a nominally first order plant with a pair of complex unmodeled poles, described by

$$y(t) = \frac{2}{(s+1)} \cdot \frac{229}{(s^2+30s+229)} [u(t)] \tag{39}$$

and a reference model

$$y_M(t) = \frac{3}{s+3} [r(t)] \tag{40}$$

The simulations were all initialized with

$$k_y(0) = -.65; \quad k_r(0) = 1.14 \tag{41}$$

which yield a stable linearization of the associated error equations. For the parameter values of eqn. (41) one finds that

$$\frac{g^*B^*(s)}{A^*(s)} = \frac{527}{s^3+31s^2+259s+527} \tag{42}$$

The reference input signal was chosen based upon the discussion of section 3.2.2

$$r(t) = .3 + 1.85 \sin 16.1t \ , \tag{43}$$

the frequency 16.1 rad/sec being the frequency at which the plant and the transfer function in (42), i.e. $\frac{g^*B^*(s)}{k_r^*A^*(s)}$, has 180° phase lag. A small d.c. offset was provided so that the linearized system would be asymptotically stable. The relatively large amplitude, 1.85 of the sinusoid in eqn. (43) was chosen so that the unstable behavior would occur over a reasonable simulation time. The adaptation gains were set equal to unity.

4.1 Sinusoidal Reference Inputs

Figure 6 shows the plant output and parameters $k_r(t)$ and $k_y(t)$ for the conditions described so far. The amplitude of the plant output at the critical frequency (ω_o=16.1 rad/sec) and the parameters grow linearly with time until the loop gain of the error system becomes larger than unity. At this point in time, even though the parameter values are well within the region of stability for the linearized system, highly unstable behavior results.

Figure 7 shows the results of a simulation, this time with the reference input

$$r(t) = .3+2.0 \sin 8.0t \tag{44}$$

This simulation demonstrates that, if the sinusoidal input is at a frequency for which the nominal controlled plant does not generate a large phase shift (at ω_o=8.0, the phase shift of eqn. (42) is -133°), the algorithm may stabilize despite the high gain operator.

Similar results were obtained for the algorithms described in [3,4,6,7,9], but are not included here due to space considerations. The reader is referred to [15] for a more comprehensive set of simulation results, in which instability occurs via both the mechanisms described in section 3.2.2 and 3.2.3, for sinusoidal inputs.

4.2 Simulations with Output Disturbances

The results in this subsection demonstrate that the instability mechanism explained in Section 3.2.2 does indeed occur when there is an additive unknown output disturbance at the wrong frequency, entering the system as shown in Fig. 1. In addition, the instability mechanism of section 3.2.3, which will drive the

algorithms unstable when there is a sinusoidal disturbance at any frequency, is also shown to take place. The same numerical example is employed here as well.

Instability via the Phase Mechanism of Section 3.2.2

In this case, CA1 was driven by a constant reference input

$$r(t) = 2.0 \tag{45}$$

with an output additive disturbance

$$d(t) = 0.5 \sin 16.1t \tag{46}$$

The results are shown in Fig. 8, and instability occurs as predicted.

Instability via the Gain Increase Mechanism of Section 3.2.3

Figure 9 shows the results of a simulation of CA1 that was generated with

$$r=2.0$$

but the disturbance was changed to

$$d(t) = 0.5 \sin 8t \tag{47}$$

At $\omega_o = 8$, $\frac{g^*B^*(s)}{k_r^*A^*(s)}$ of eqn. (42) provides only -133° phase shift so the sinusoidal error signal of increasing amplitude, which is characteristic of instability via the mechanism of Section 3.2.2, is not seen in Fig. 9. What is seen is that the system becomes unstable by the mechanism of Section 3.2.3. While the output appears to settle down to a steady state sinusoidal error, the k_y parameter drifts away until the point where the controller becomes unstable. (Only the onset of unstable behavior is shown in Figure 9 in order to maintain scale).

The most disconcerting part of this analysis is that none of the systems analyzed have been able to counter this parameter drift for a sinusoidal disturbance at any frequency tried!

Indeed, Figure 10 shows the results of a simulation run with reference input

$$r = 0.0 \tag{48}$$

and constant disturbance

$$d = 3.0 \tag{49}$$

The simulation results show that the output settles for a long time with non-zero error but the parameter k_y increases in magnitude until instability ensues. Thus the adaptive algorithm shows no ability to act even as a regulator when there are output disturbances.

However, in order to drive the system unstable with a constant disturbance in the same order of magnitude of time as it took to drive the system unstable with a higher frequency sinusoid, the magnitude of the disturbance must be much larger in the constant disturbance case. The constant disturbance must be larger because the nominal control system has a larger gain at d.c. and thus better disturbance rejection. The time it takes for the system to go unstable is inversely proportional to the square of the magnitude of the part of disturbance still present at the output of the closed-loop controlled system.

In the previous simulations the unmodeled dynamics which were used were highly damped. Figure 11 shows the results of a simulation of a plant with less well damped unmodeled dynamics at a somewhat lower frequency and a smaller disturbance. The plant used in the run is described by

$$y(t) = \frac{2}{s+1} \cdot \frac{100}{s^2+8s+100} [u(t)] \tag{50}$$

The reference input was again

$$r(t) = 2.0 \tag{51}$$

The disturbance used was

$$d(t) = 0.1 \sin 8t \tag{52}$$

In this case the parameter drift is slower than in Figure 9. However, the parameters need not drift as far to cause instability due to the less benign unmodeled dynamics in this case, so the system exhibits unstable behavior in approximately the same amount of time.

It is important to understand that the parameters will drift and cause instability no matter how small the disturbance. If the disturbance is small, the parameters will drift slowly and the system will take a long time to become unstable but it will indeed become unstable if the disturbance persists long enough.

5. CONCLUSIONS

In this paper it was shown, by analytical methods and verified by simulation results, that existing adaptive algorithms as described in [1-4,6,7,19], have imbedded in their adaptation mechanisms infinite gain operators which, in the presence of unmodeled dynamics, will cause:

- instability, if the reference input is a high frequency sinusoid
- instability, if there is a sinusoidal output disturbance at any frequency including d.c.
- instability, at any frequency of reference inputs for which there is a non-zero steady state error.

While the first problem can be alleviated by proper limitations on the class of permissible reference inputs, the designer has no control over the additive output disturbances which impact his system, or of non-zero steady-state errors that are a consequence of imperfect model matching. Sinusoidal disturbances and inexact matching conditions are extremely common in practice and can produce disastrous instabilities in the adaptive algorithms considered.

Suggested remedies in the literature such as low pass filtering of plant output or error signal [26,7,21] will not work either. It is shown in [15] that adding the filter to the output of the plant does nothing to change the basic stability problem as discussed in section 3.2. It is also shown in [15] that filtering of the output error merely results in the destabilizing input being at a lower frequency.

Exactly analogous results were also obtained for discrete-time algorithms as described in [5,17,18,20] and have been reported in [15].

Finally, unless something is done to eliminate the adverse reaction to disturbances-at any frequency-and to nonzero steady-state errors in the presence of unmodeled dynamics, the existing adaptive algorithms cannot be considered as serious practical alternatives to other methods of control.

ACKNOWLEDGEMENT

The authors wish to thank Bernie Cyr [24] and Peter Kokotovic who brought to our attention errors in the simulation results originally presented in [15] and [25] so that they could be corrected for this paper.

6. REFERENCES

1. K.S. Narendra and L.S. Valavani, "Stable Adaptive Controller Design-Direct Control," IEEE Trans. Autom. Contr., Vol. AC-23, pp. 570-583, Aug. 1978.

2. A. Feuer and A.S. Morse, "Adaptive Control of Single-Input Single-Output Linear Systems," IEEE Trans. Autom. Contr., Vol. AC-23, pp. 557-570, August 1978.

3. K.S. Narendra, Y.H. Lin and L.S. Valavani, "Stable Adaptive Controller Design, Part II: Proof of Stability," IEEE Trans. Autom. Contr., Vol. AC-25, pp. 440-448, June 1980.

4. A.S. Morse, "Global Stability of Parameter Adaptive Control Systems," IEEE Trans. Autom. Contr., Vol. AC-25, pp. 433-440, June 1980.

5. G.C. Goodwin, P.J. Ramadge, and P.E. Caines, "Discrete-Time Multivariable Adaptive Control," IEEE Trans. Autom. Contr., Vol. AC-25, pp. 449-456, June 1980.

6. I.D. Landau and H.M. Silveira, "A Stability Theorem with Applications to Adaptive Control," IEEE Trans. Autom. Contr., Vol. AC-24, pp. 305-312, April 1979.

7. B. Egardt, "Stability Analysis of Continuous-Time Adaptive Control Systems," SIAM J. of Control and Optimization, Vol. 18, No. 5, pp. 540-557, Sept., 1980.

8. L.S. Valavani, "Stability and Convergence of Adaptive Control Algorithms: A Survey and Some New Results," Proc. of the JACC Conf., San Francisco, CA, August 1980.

9. B. Egardt, "Unification of Some Continuous-Time Adaptive Control Schemes," IEEE Trans. Autom. Contr., Vol. AC-24, No. 4, pp. 588-592, August 1979.

10. P.A. Ioannou and P.V. Kokotovic, "Error Bound for Model-Plant Mismatch in Identifiers and Adaptive Observers," IEEE Trans. Autom. Contr., Vol. AC-27, pp. 921-927, August 1982.

11. C. Rohrs, L. Valavani, M. Athans, and G. Stein, "Analytical Verification of Undesirable Properties of Direct Model Reference Adaptive Control Algorithms," LIDS-P-1122, M.I.T., August 1981; also Proc. 20th IEEE Conf. on Decision and Control, San Diego, CA, December 1981.

12. P. Ioannou and P.V. Kokotovic, "Singular Perturbations and Robust Redesign of Adaptive Control," Proc. of 21st. IEEE Conf. on Decision and Control, Orlando, FL, Dec. 1982, pp. 24-29.

13. C. Rohrs, L. Valavani and M. Athans, "Convergence Studies of Adaptive Control Algorithms, Part I: Analysis," Proc. IEEE CDC Conf., Albuquerque, New Mexico, 1980, pp. 1138-1141.

14. R.V. Monopoli, "Model Reference Adaptive Control with an Augmented Error Signal," IEEE Trans. Autom. Contr., Vol. AC-19, pp. 474-484, October 1974.

15. C. Rohrs, Adaptive Control in the Presence of Unmodeled Dynamics, Ph.D. Thesis, Dept. of Elec. Eng. and Computer Science, M.I.T., August 1982.

16. P. Ioannou, Robustness of Model Reference Adaptive Schemes with Respect to Modeling Errors, Ph.D. Thesis, Dept. of Elec. Eng., Univ. of Illinois at Report DC-53, August 1982.

17. B. Egardt, "Unification of Some Discrete-Time Adaptive Control Schemes," IEEE Trans. Autom. Contr., Vol. AC-25, No. 4, pp. 693-697, August 1980.

18. K.J. Åström, and B. Wittenmark, "A Self-Tuning Regulator," Automatica, No. 8, pp. 185-199, 1973.

19. G. Kreisselmeier, "Adaptive Control via Adaptive Observation and Asymptotic Feedback Matrix Synthesis," IEEE Trans. Autom. Contr., Vol. AC-25, pp. 717-722, August 1980.

20. I.D. Landau, "An Extension of a Stability Theorem Applicable to Adaptive Control," IEEE Trans. Autom. Contr., Vol. AC-25, pp. 814-817, August 1980.

21. I.D. Landau, and R. Lozano, "Unification of Discrete-Time Explicit Model Reference Adaptive Control Design," Automatica, Vol. 17, No. 4, pp. 593-611, July 1981.

22. K.S. Narendra and Y.H. Lin, "Stable Discrete Adaptive Control," IEEE Trans. Autom. Contr., Vol. AC-25, No. 3, pp. 456-461, June 1980.

23. R.L. Kosut and B. Friedlander, "Performance Robustness Properties of Adaptive Control Systems," Proceeding of 21st. IEEE Conf. on Decision and Control, Orlando, FL, Dec. 1982, pp. 18-23.

24. B. Cyr, Instability and Stabilization of an Adaptive System, Decision and Control Laboratory, Report DC-60, Univ. of Illinois, December 1982.

25. C.E. Rohrs, L. Valavani, M. Athans, and G. Stein, "Robustness of Adaptive Control Algorithms in the Presence of Unmodeled Dynamics," Proc. 21st. IEEE Conf. on Decision and Control, Orlando, FL, Dec. 1982, pp. 3-11.

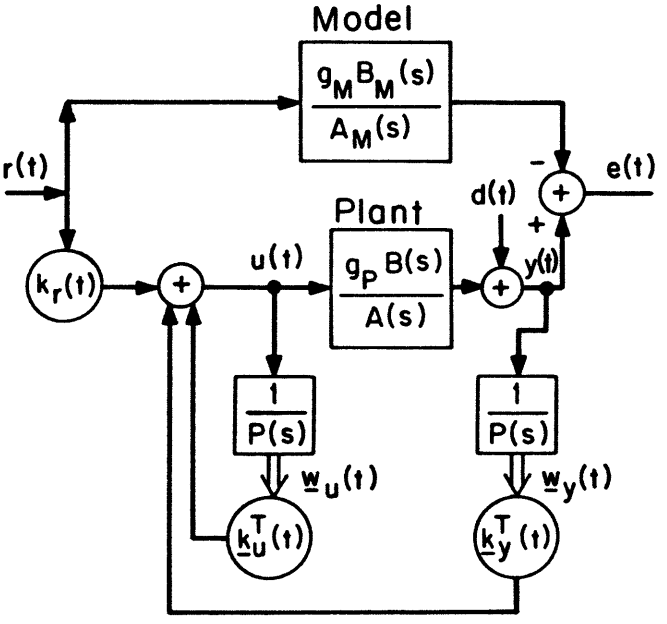

FIGURE 1: Controller structure of CA1 with additive output disturbance, d(t).

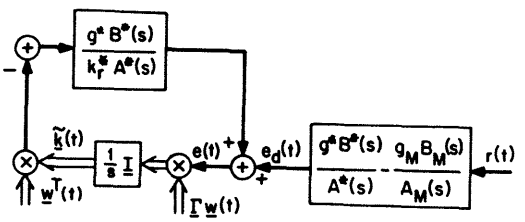

FIGURE 2: Error System for CA1.

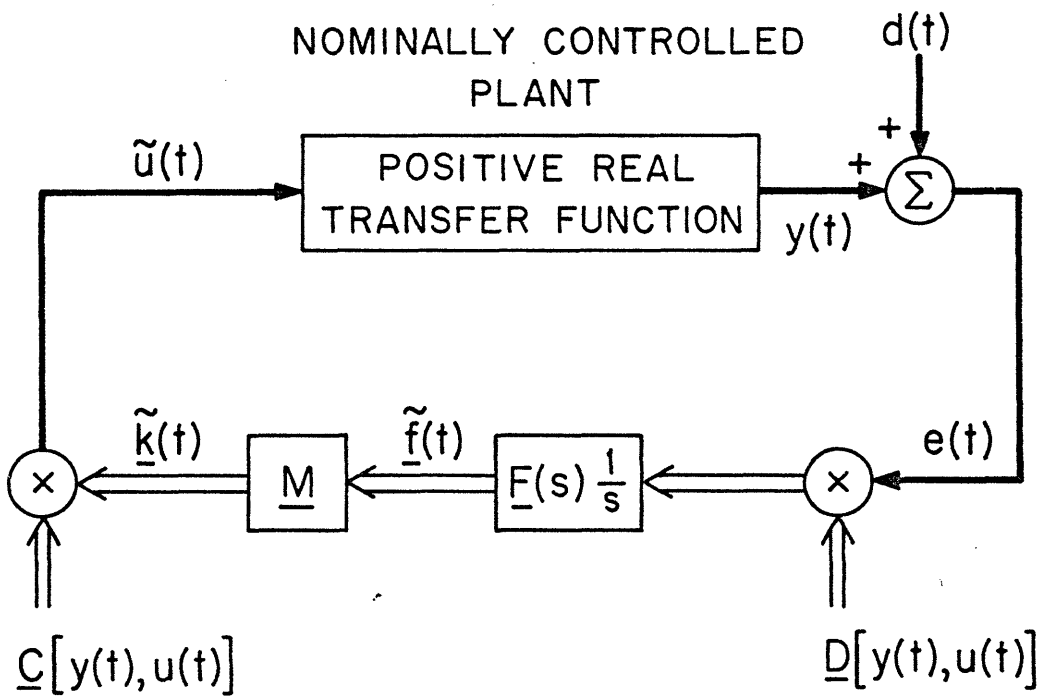
NOMINALLY CONTROLLED
PLANT
d(t)
+
+
ũ(t)
POSITIVE REAL
TRANSFER FUNCTION
y(t)
Σ
k̃(t)
f̃(t)
e(t)
M
F(s) 1/s
C[y(t),u(t)]
D[y(t),u(t)]

FIGURE 3:

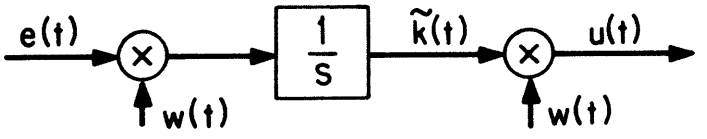

FIGURE 4: Infinite gain operator of CA1.

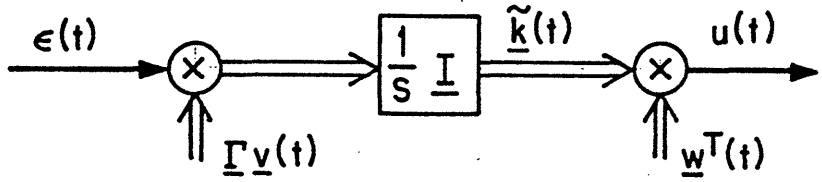

Figure 5a. The infinite gain operator of CA2.

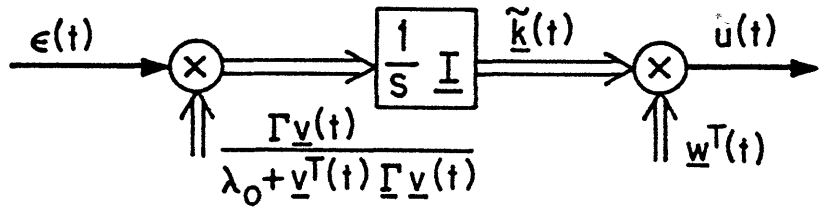

Figure 5b. The infinite gain operator CA3.

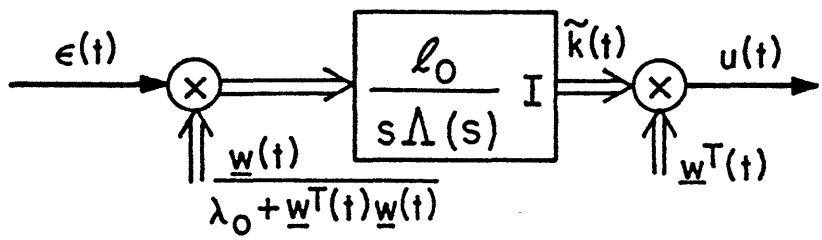

Figure 5c. The infinite gain operator CA4.

Figure 5: The infinite gain operators of CA2, CA3, and CA4.

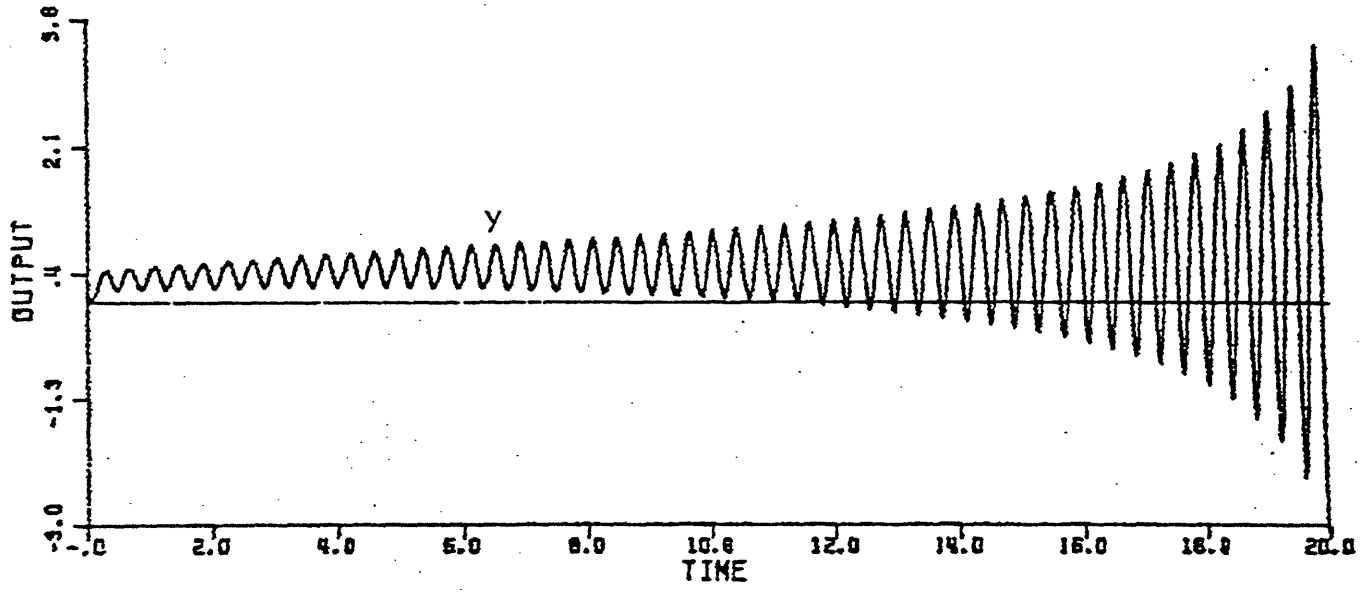

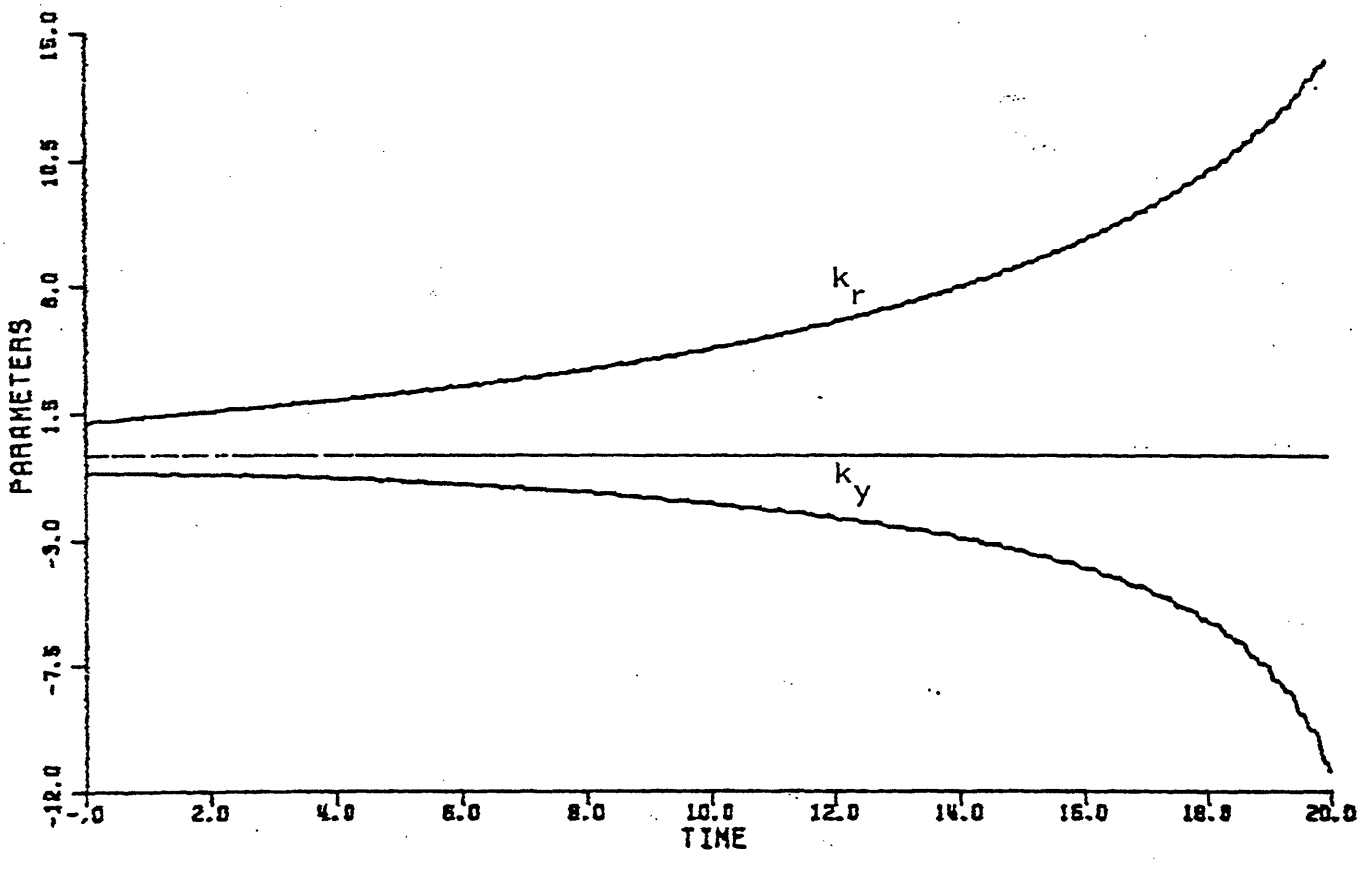

FIGURE 6: Simulation of CA1 with unmodeled dynamics and $r(t)=0.3 + 1.85\sin 16.1t$ (System eventually becomes unstable.)

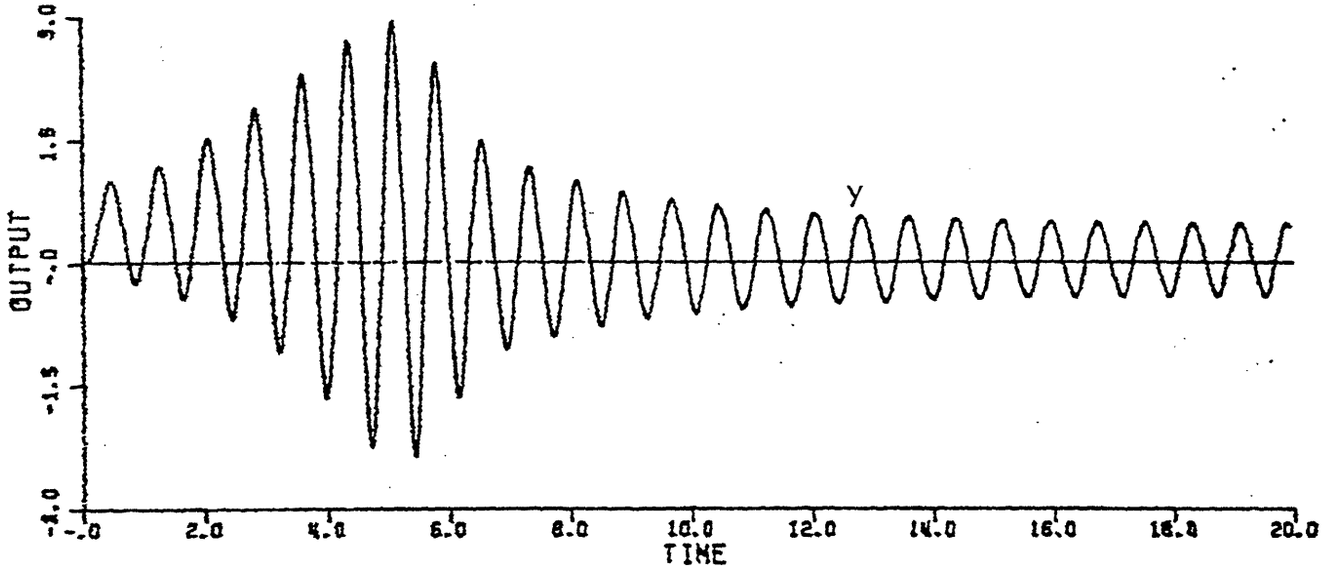

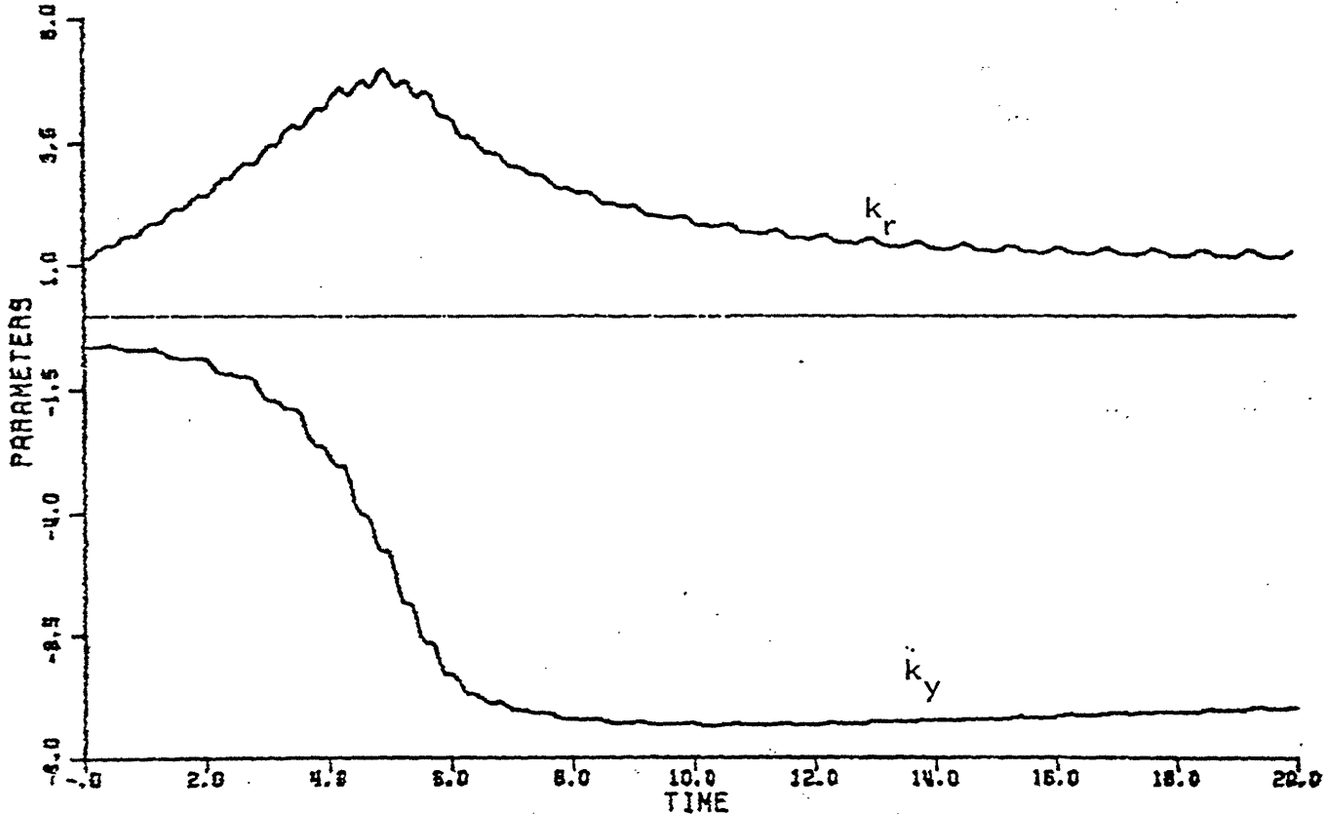

FIGURE 7: . .Simulation of CA1 with unmodeled dynamics and $r(t)=0.3 + 2.0\sin 8.0t$

(No instability observed).

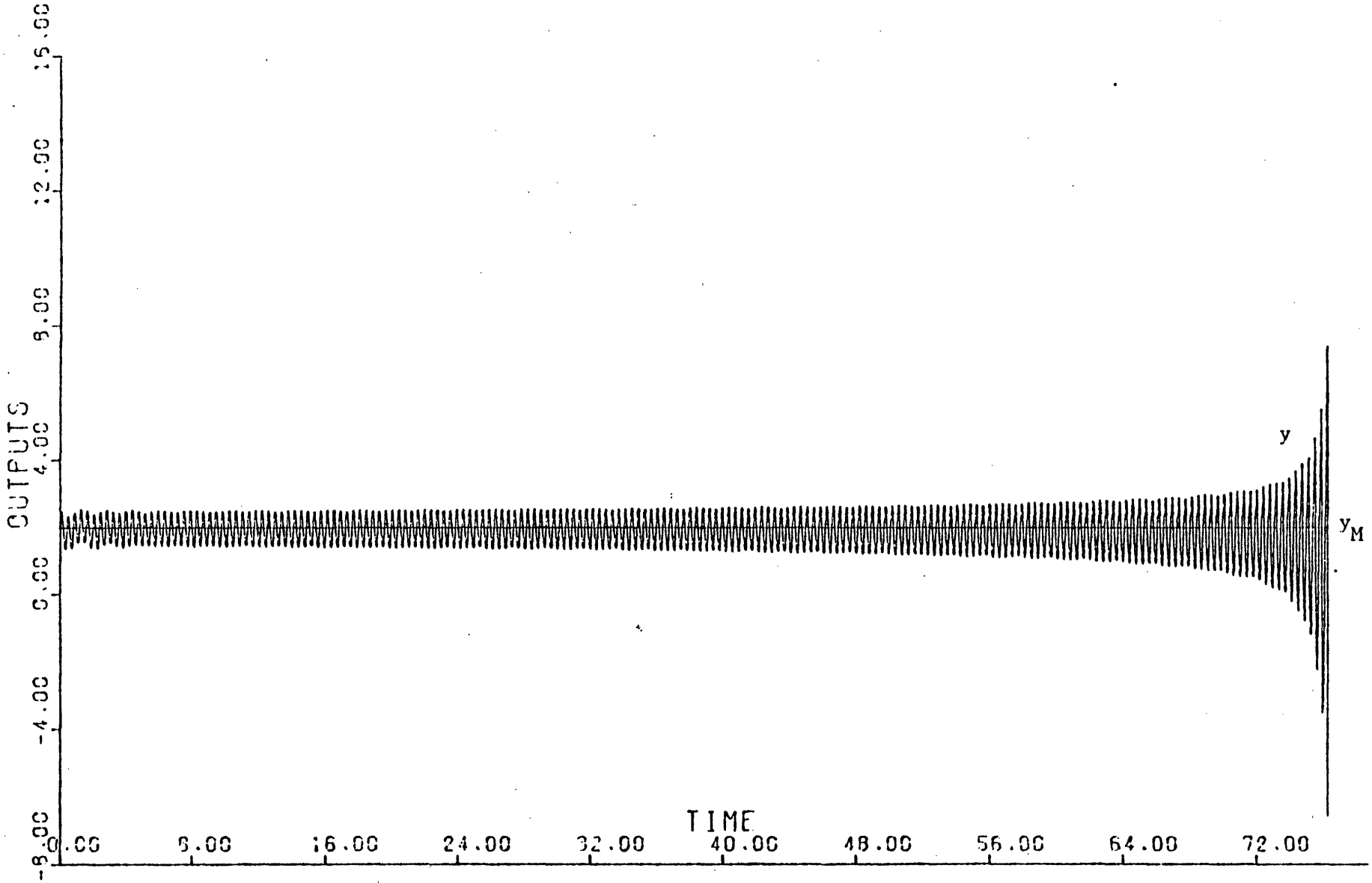

FIGURE 8a: Simulation of CA1 with highly damped unmodeled dynamics, r(t)=2.0 and d(t) = 0.5sin16.1t.

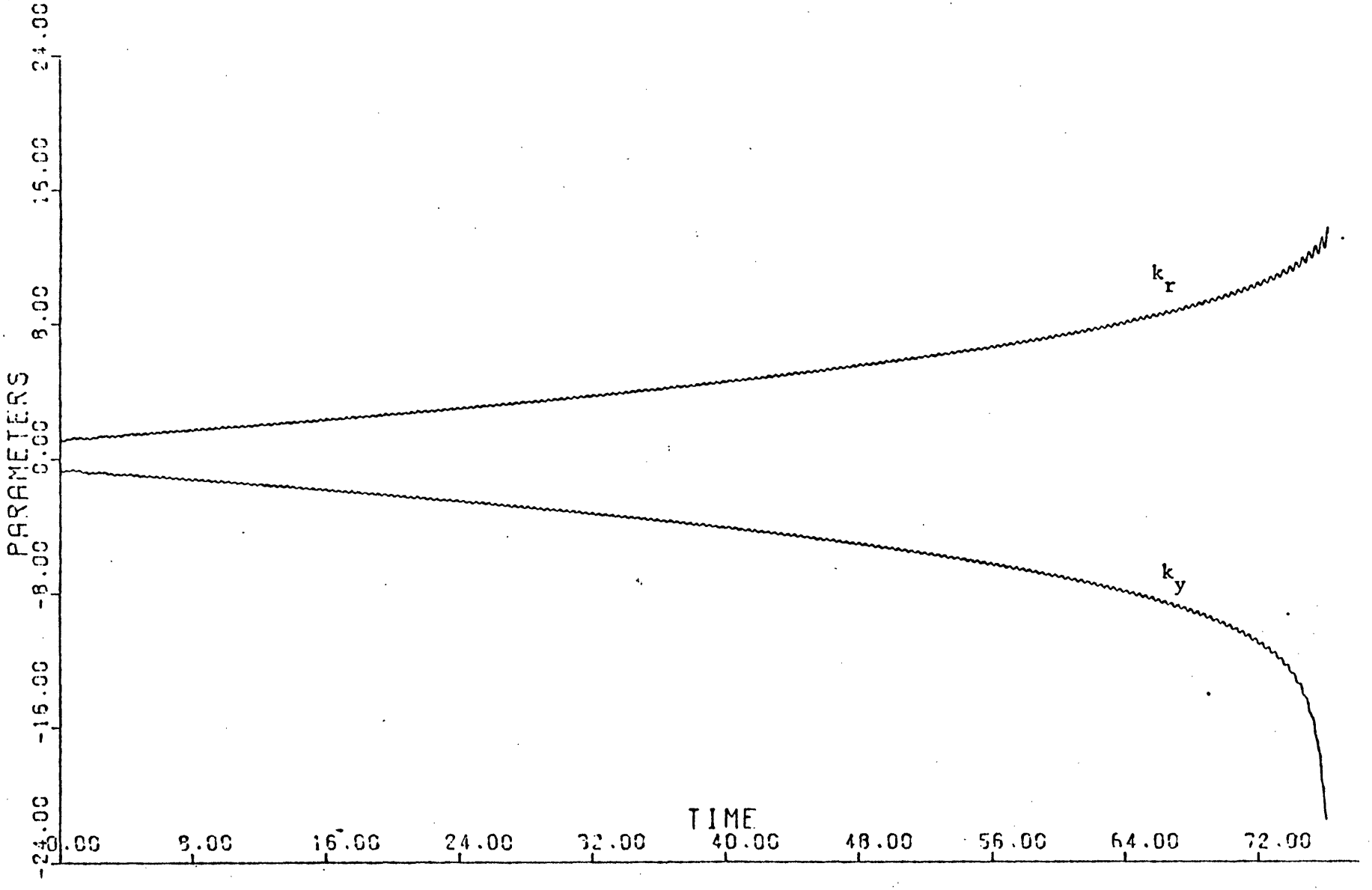

FIGURE 8b: Simulation of CA1 with highly damped unmodeled dynamics, r(t)=2.0 and d(t) = 0.5sin16.1t.

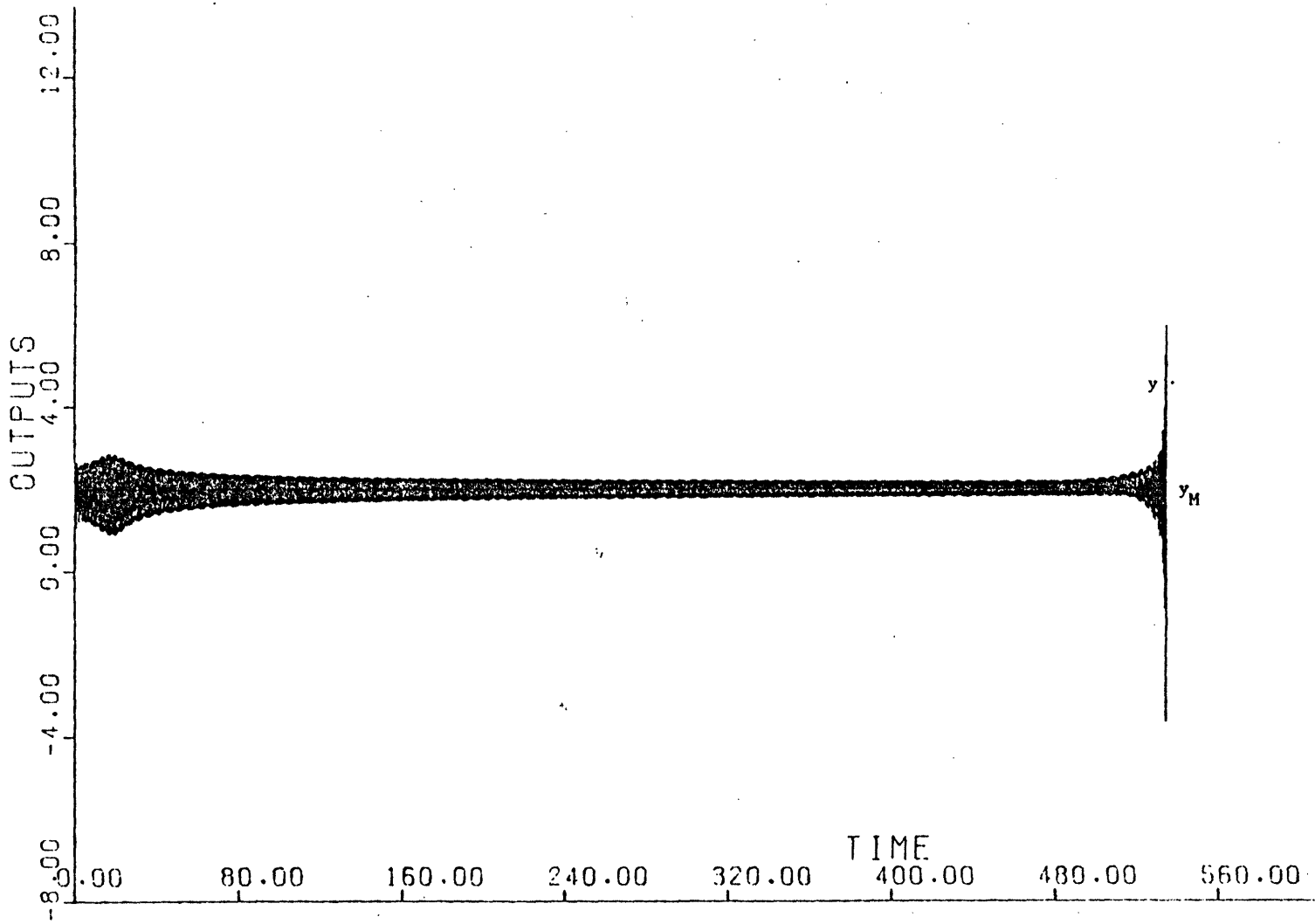

FIGURE 9a: Simulation of CAl with highly damped unmodeld dynamics, r(t)=2.0 and d(t)=0.5sin8t.

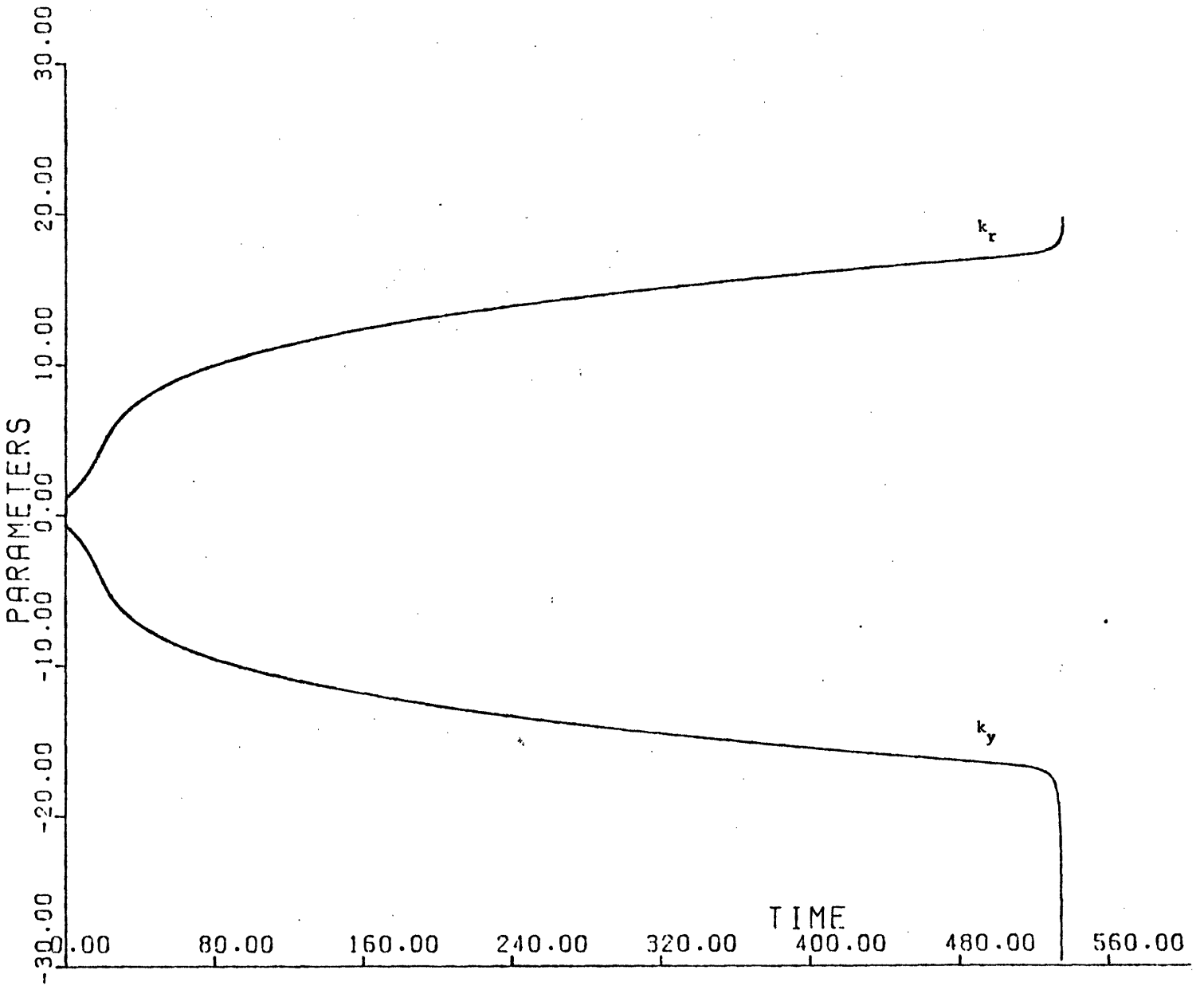

FIGURE 9b: Simulation of CA1 with highly damped unmodeled dynamics, r(t)=2.0 and d(t)=0.5sin8t.

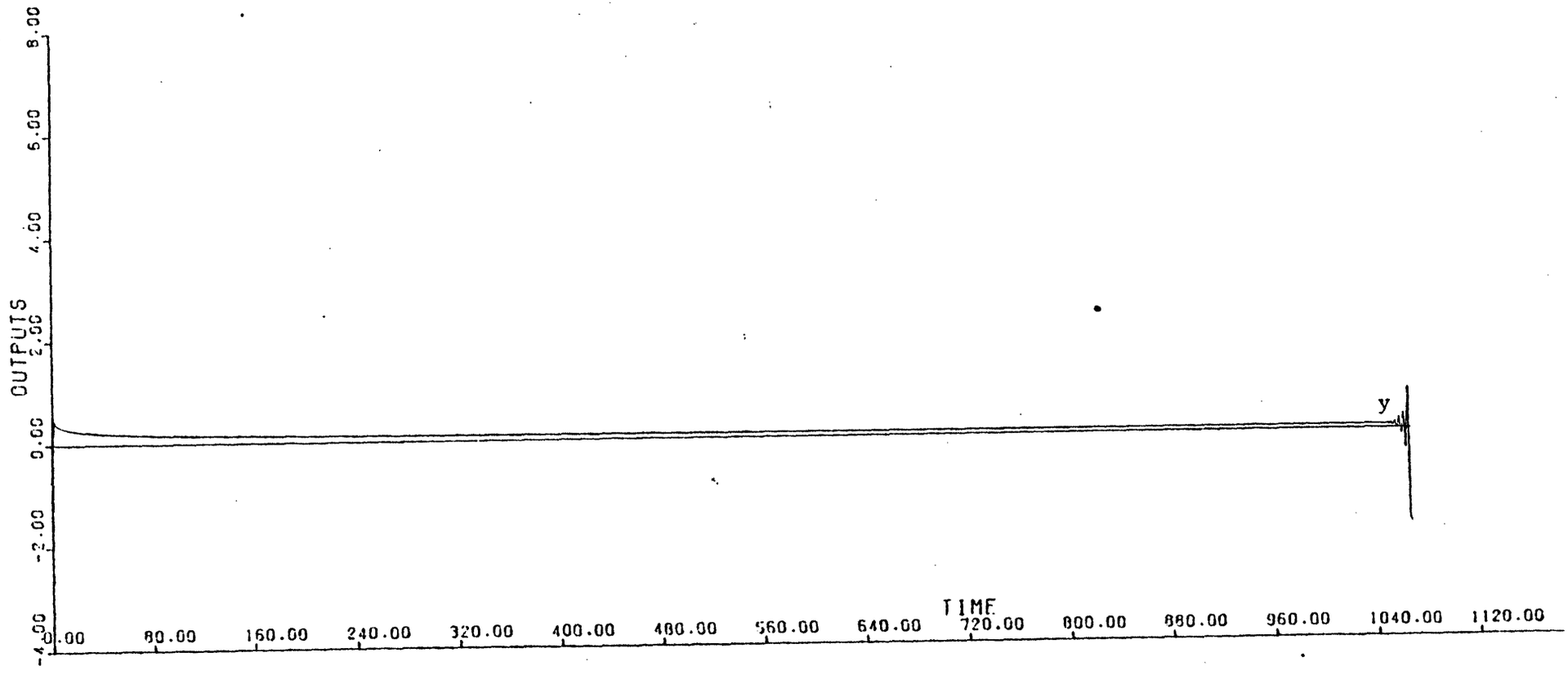

FIGURE 10a: Simulation of CA1 with highly damped unmodeled dynamics, $r(t)=0.0$ and $d(t)=3.0$ (system becomes unstable).

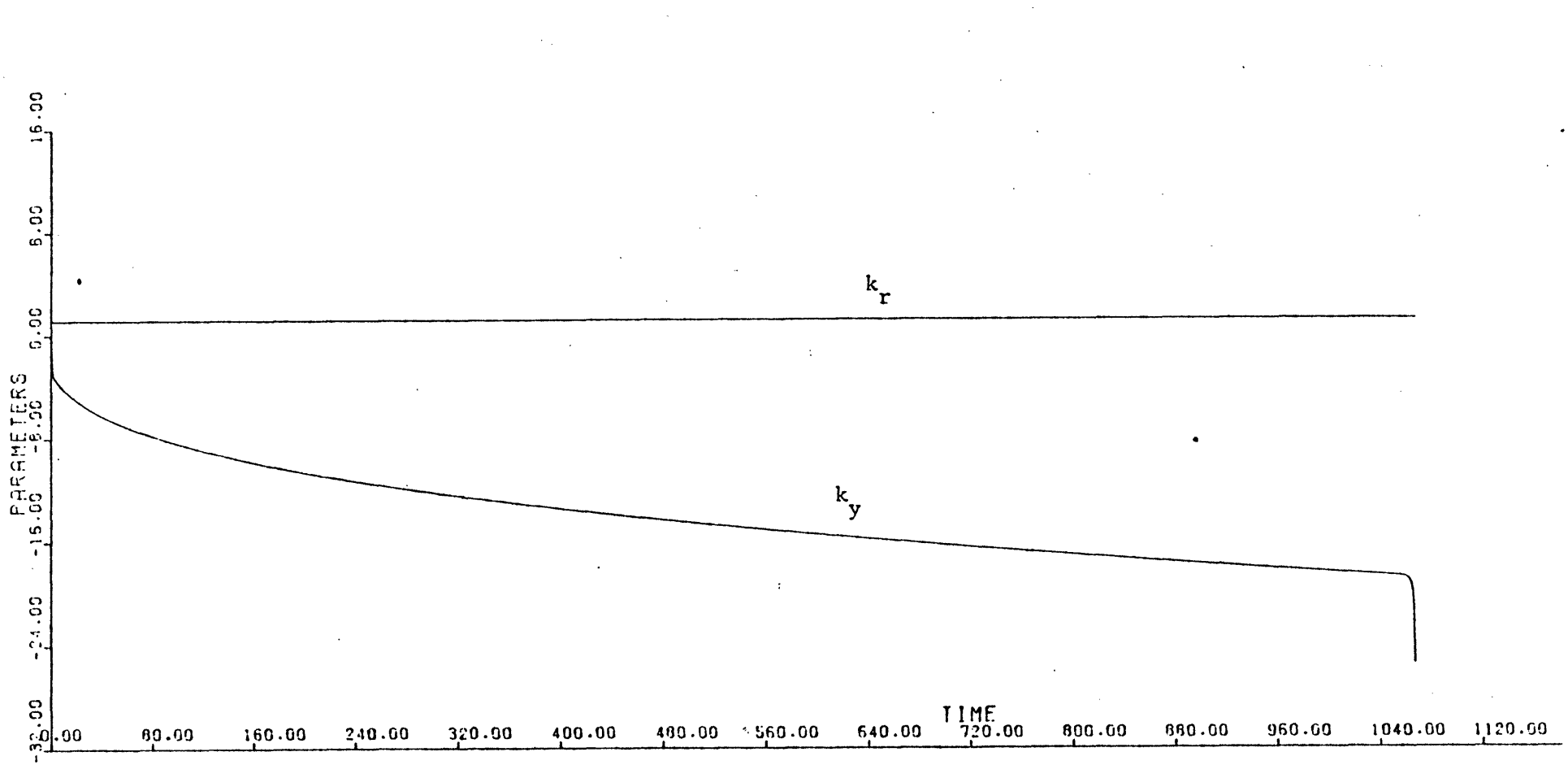

FIGURE 10b: Simulation of CA1 with highly damped unmodeled dynamics, r(t)=0.0 and d(t)=3.0 (system becomes unstable).

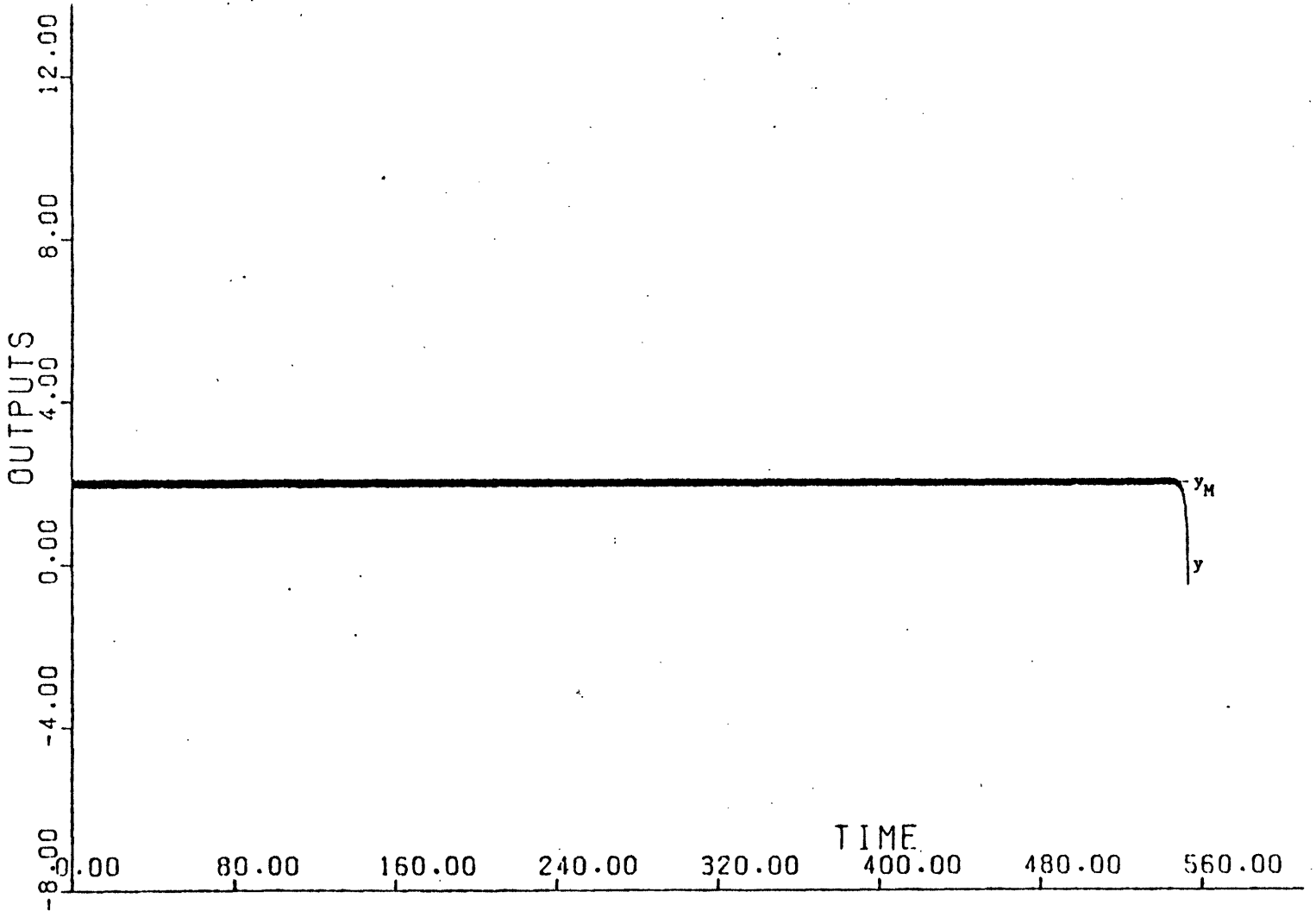

FIGURE 11a: Simulation of CA1 with poorly damped unmodeled dynamics, r(t)=2.0 and d(t)=0.1sin8t.

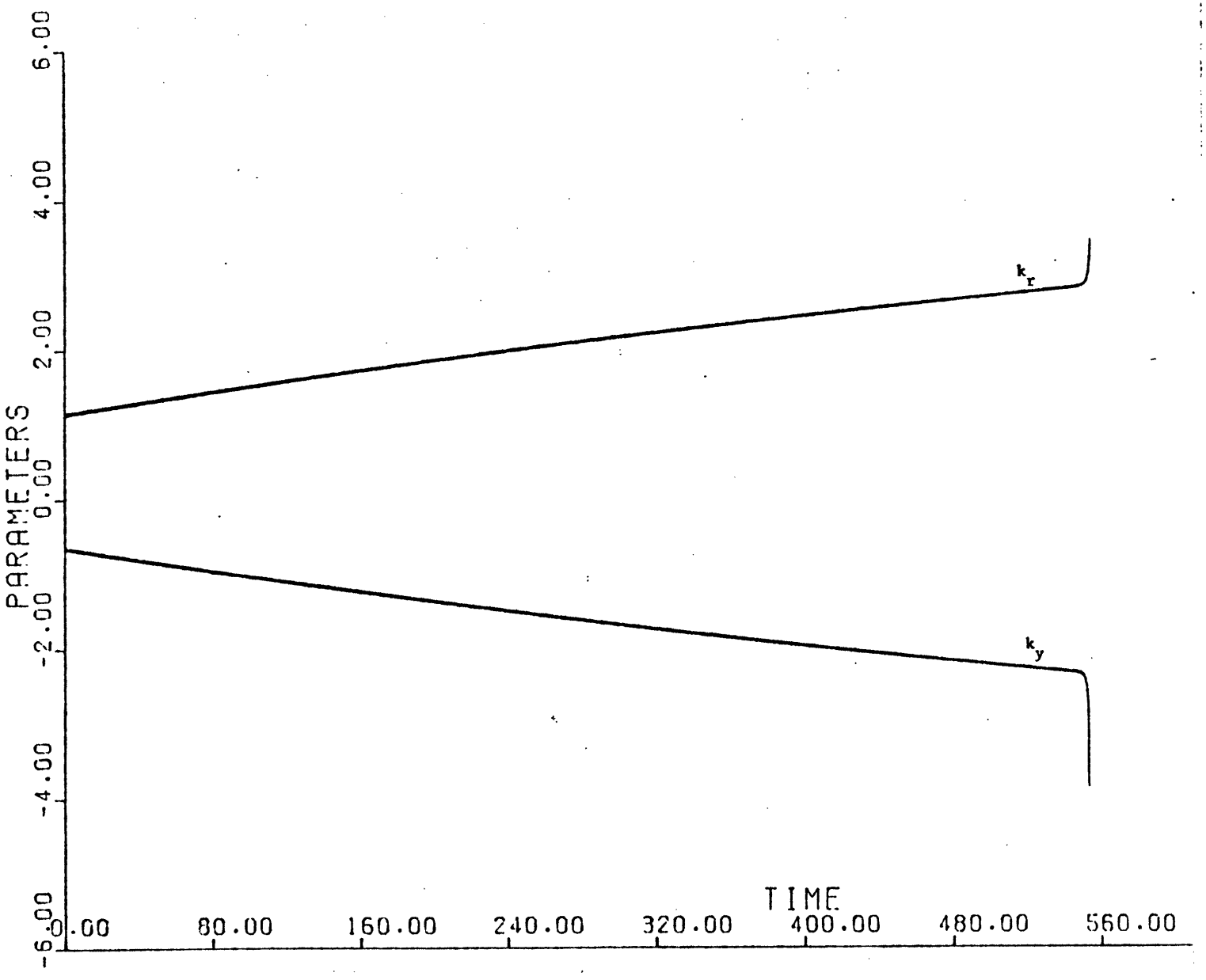

FIGURE 11b: Simulation of CA1 with poorly damped unmodeled dynamics, r(t)=2.0 and d(t)=0.1sin8t.